European Cells and Materials Vol. 21 2011 (pages 1-14) DOI: 10.22203/eCM.v021a01 ISSN 1473-2262

CHONDROITIN SULPHATE SULPHATION MOTIF EXPRESSION IN THE ONTOGENY OF THE INTERVERTEBRAL DISC

A.J. Hayes, C.E. Hughes, J.R. Ralphs* and B. Caterson

Connective Tissue Biology Laboratory and Cardiff Institute of Tissue Engineering and Repair, Cardiff School of Biosciences, Cardiff University, Cardiff CF10 3US, Wales, UK

Abstract

Chondroitin sulphate chains on cell and extracellular matrix proteoglycans play important regulatory roles in developing systems. Specific, developmentally regulated, sulphation motifs within the chondroitin glycosaminoglycan structure may help bind, sequester or present bioactive signalling molecules to cells thus modulating their behaviour. Using monoclonal antibodies 3B3(-), 4C3, 6C3 and 7D4, we have mapped the distribution of different chondroitin sulphation epitopes in a rat intervertebral disc developmental series. The sulphation epitopes had complex, dynamic and specific distributions in the disc and vertebral tissues during their differentiation, growth and ageing. At embryonic day [E]15, prior to disc differentiation, 4C3 and 7D4 occurred within the cellular disc condensations whilst 6C3 was present in the notochordal sheath. At E17, post disc differentiation, 4C3 and 7D4 occurred within the nucleus pulposus, inner annulus and vertebral bodies; 3B3(-) in the nucleus, inner annulus, annulus/vertebral body interface and perichondrium; and 6C3, ventrally, within the perichondrium. At E19, 3B3(-), 4C3 and 7D4 became further restricted to the nucleus, inner annulus, annulus/vertebral body interface and perichondrium. Prior to birth, all four epitopes occurred within the inner annulus and nucleus, with 6C3 and 7D4 also occurring within the future end-plate. Postnatal expression of the sulphation epitopes was more widespread in the disc and also within the growth plate. At 4 months, the epitopes were associated with chondrocyte clusters within the nucleus; and at 24 months, with annular lesions. Overall, our data suggests that differential sulphation of chondroitin correlates with significant events in development, growth and aging of the rat intervertebral disc.

Keywords: Intervertebral disc, vertebral body, growth plate, chondroitin sulphate, sulphation motif, differentiation, development, growth, ageing.

*Address for correspondence:
J. Ralphs
Connective Tissue Biology Laboratory and Cardiff Institute of Tissue Engineering and Repair,
Cardiff School of Biosciences, Cardiff University,
Cardiff CF10 3US, Wales, UK
Telephone Number: ++44 (0)29 874954
FAX Number: +44 (0)2920 874594
E-mail: ralphs@cf.ac.uk

Introduction

The intervertebral disc (IVD) functions as a biomechanical shock absorber within the vertebral column. It consists of three intimately associated tissues; the annulus fibrosus, the nucleus pulposus and the cartilage end-plates. The annulus encloses the nucleus pulposus circumferentially and is strongly attached to the cartilage end plates of the vertebral bodies. The macromolecular composition and organisation of the different discal tissues reflect their unique origins and the different roles they play in disc function (Rufai *et al*., 1995; Hayes *et al*., 2001). The annulus consists of lamellae of oriented collagen bundles organised into a cross-ply structure that allows twisting and bending movements of the spine whilst resisting radial forces exerted by the nucleus in response to compression. The outer part of the annulus is fibrous and has a high content of type I collagen; whilst the inner part is fibrocartilaginous and has more type II collagen and a higher proteoglycan (PG) content. The nucleus is less organised than the annulus and is more cartilaginous, containing mainly type II collagen and having the highest PG and water content (Bogduk, 2005).

The IVD undergoes dramatic changes during development, growth and ageing (Peacock, 1951a,b; Walmsley, 1953; Rufai *et al*., 1995; Hayes *et al*., 2001). It is formed from two distinct tissues during early foetal development: the embryonic notochord and sclerotomally-derived mesenchyme. Initially, the mesenchymal cells surround the notochord and form regular repeating dense annular condensations of cells interspersed with more widely-spaced cartilage precursor cells of the early developing vertebral bodies (Fig. 1). As the vertebral body cartilage differentiates, the annular condensations shows evidence of differentiation into inner and outer regions. Shortly afterwards, the notochord rapidly bulges in the region of the developing disc, and thins in the vertebral bodies, from which it eventually disappears (Fig. 2). The bulges form the foetal nucleus pulposus, and as they enlarge the annular condensations differentiate into the cartilaginous inner and fibrous outer annulus fibrosus, the ends of the vertebral bodies on each side later forming the cartilage endplates. Post-natally, the disc enlarges considerably with skeletal growth by accumulation of extracellular matrix (ECM): the annulus fibrosus becomes highly lamellar and the boundary between inner and outer annulus becomes less distinct; as does the interface between inner annulus and nucleus pulposus, as the nucleus starts to fill in with cartilaginous ECM (Fig. 3). A feature of this process is the appearance of clusters of chondrocyte-like cells that occur towards the margins of the nucleus (Rufai *et al*., 1995; Johnson *et*

al., 2001; Sharp *et al*., 2009). Despite their dissimilarity, these cells are said to derive from notochordal precursors (Risbud *et al*., 2010). During ageing the IVD becomes progressively more fibrous and disorganised in appearance with overt signs of degeneration including annular tears, calcification and osteophytosis (Fig. 4).

Chondroitin sulphate (CS) glycosaminoglycan (GAG) chains on cell-associated and ECM PGs play important roles in the development and biological function of the IVD (Hayes *et al*., 2001). CS is composed of repeating disaccharide units of glucuronic acid and N-acetylgalactosamine. The hydroxyl groups on these disaccharide units can be differentially sulphated, yielding considerable structural heterogeneity within the CS chains. Due to their high content of sulphate and carboxyl groups CS chains have a strong negative charge, thus an inherent ability to attract positively charged matrix molecules through electrostatic interaction. As a result they contribute to the water-binding capacity of PGs via their ionic, carboxyl and sulphate radicals and, therefore, are important to the hydrodynamic properties of the disc in resisting biomechanical load (Urban and Maroudas, 1980; Bogduk, 2005). In addition to this, CS and heparan sulphate (HS) chains on PGs can interact in a highly specific manner with a wide variety of matrix molecules (e.g., growth factors, cytokines, morphogens, chemokines and enzymes) via unique sulphation sequence motifs occurring within their chains (reviewed in detail by Handel *et al*., 2005; Raman *et al*., 2005; Sasisekharan *et al*., 2006; Gandhi and Mancera, 2008; Merry and Astrautsova, 2008). GAG chains on PGs thus have the potential to influence many cell behaviours in the disc including cell proliferation, differentiation, migration, and matrix secretion (for example, Deepa *et al*., 2002; Kawashima *et al*., 2002; Nandini *et al*., 2004; Klüppel *et al*., 2005; Tiedemann *et al*., 2005; Smith *et al*., 2007; Cortes *et al*., 2009; Alliston *et al*., 2010; Gualeni *et al*., 2010).

Earlier studies (Sorrell *et al*., 1988; Sorrell and Caterson, 1989; Sorrell *et al*., 1990; Sorrell *et al*., 1996; Caterson *et al*., 1990; Mark *et al*., 1989; Mark *et al*., 1990) using monoclonal antibodies (mAbs) towards unique native sulphation motif epitopes present on CS chains on PGs have shown that differential CS sulphation is involved in the development of a wide range of connective tissues during embryogenesis. Of relevance, CS sulphation motif epitopes recognised by mAbs MC21C (Mark *et al*., 1989), 3B3(-) and 7D4 (Hayes *et al*., 2001) are associated with the early development of the axial skeleton and IVD, where they appear to occur at developmentally important sites of tissue growth, differentiation and interaction. Furthermore, the CS epitopes recognised by the latter two antibodies have been shown to occur in degenerate human discs, where it is thought they may be involved in cellular reparatory processes (Roberts *et al*., 1994; Johnson *et al*., 2001). Thus, there is compelling evidence to suggest that chondroitin sulphation may play a significant role in the development, growth, and aging of the IVD.

In this study, to better understand the role of CS sulphation in the ontogeny of the IVD, we map the spatio-temporal distribution of four distinct native CS sulphation motif epitopes in a rat disc developmental series from the onset of initial disc histogenesis, at E15, to the onset of age-related degeneration and attempted repair, at 24 months. We show interesting dynamics of CS motif expression in the developing structures of the disc and vertebral bodies that relate to their differentiation, growth and homeostasis. Overall, our data indicates that CS sulphation motifs on cell and ECM PGs have significant involvement in the ontogeny of the IVD and may play roles in the binding of soluble signalling molecules, such as growth factors, cytokines, morphogens and chemokines.

Materials and Methods

Source of material

Archived, wax embedded spinal tissue was obtained from foetal (E15-E21), adult (4 month) and aged (24 month) white Wistar rats under humane conditions. Foetal spines were processed *in situ*, whereas L1-L2 IVDs were dissected from adult and aged spines prior to fixation and histological processing.

Histological processing

Tissues were fixed in 10% neutral buffered formol saline, decalcified (from E19 onwards) in 2% nitric acid until radiologically clear, and then processed into paraffin wax using standard histological methods. Serial sections were cut through the vertebral column in the sagittal plane and 6μm sections collected onto Histobond glass histology slides (R.A. Lamb, now Fisher Scientific, Loughborough, UK). Tissue sections were de-waxed and rehydrated prior to all immunohistochemical labelling procedures. Sections were immunohistochemically labelled using an indirect immunoperoxidase labelling method (see below). To facilitate direct comparison of antibody labelling patterns, consecutive serial sections were used whenever possible and the same lumbar disc was followed throughout foetal development. For comparative analysis of CS sulphation patterns in 4 and 24 month specimens, identical regions of discal tissues were photographed as shown in Figs. 5 and 6.

Immunoperoxidase labelling procedure

After de-waxing and rehydrating, tissue sections were circumscribed with water repellent ink using a Dako delimiting pen (Dako, Glostrup, Denmark) prior to immunohistochemical labelling. Immunoperoxidase labelling was with the Vector ABC universal immunoperoxidase labelling kit (Vector Laboratories, Burlingame, CA, USA) using a panel of monoclonal antibodies towards sulphation motif epitopes present in native CS GAG chains (refer to Table 1). To block endogenous peroxidase activity sections were first immersed in 0.3% hydrogen peroxide in water (v/v) for 1 hour. After washing in water, sections were blocked in horse-serum for 30 min to prevent non-specific labelling. Sections were then incubated overnight at 4°C with each of the monoclonal antibodies. Controls were incubated with non-immune mouse immunoglobulins or the primary

Table 1. Antibodies used in immunohistochemistry

Antibody	Clone (Isotype)	Dilution	Specificity ‡	References
3B3(-)†	Monoclonal (IgM, κ)	1:20	Terminal disaccharide of CS chains: 6-sulphated galactosamine adjacent to a terminal glucuronate.	Sorrell *et al.*, 1988, 1990, 1996; Hardingham *et al.*, 1994;
4C3	Monoclonal (IgM, κ)	1:20	Distinct, as yet unidentified, native CS sulphation motif epitopes occurring towards linkage region.	Caterson *et al.*, 1990.
7D4	Monoclonal (IgM, κ)	1:20		
6C3	Monoclonal (IgM, κ)	1:20	Unidentified sulphation motif occurring towards non-reducing terminus.	

† (-) denotes use of antibody without chondroitinase ABC pre-treatment. The same antibody can be used to detect chondroitin-6-sulphate 'stubs' after chondroitinase ABC pre-digestion *i.e.* 3B3(+). ‡ Data based on CS chains of aggrecan.

antibody was omitted and replaced with phosphate buffered saline (PBS), pH 7.4. All immunolabelling controls were negative showing no non-specific antibody labelling. After overnight incubation in primary antibody, sections were washed in PBS (3 x 5 min) and then incubated with biotinylated secondary antibody for 30 min at room temperature, washed again (3 x 5 min), and then incubated with the avidin, biotin complex for 30 min. After another wash in buffer (3 x 5 min), NovaRed peroxidase substrate (Vector Laboratories) was added to the sections until the desired colour intensity was developed. Sections were then washed in water, counterstained with haematoxylin for nuclear context and mounted under coverslips with DPX mountant.

Microscopy

IVDs from the lumbar region of the foetal spine and L1-L2 discs from adults and aged rats (Figs. 5 and 6) were observed and photographed on a Leica DM6000 microscope (Leica Microsystems, Heidelberg, Germany) under both brightfield and differential interference contrast (DIC) optics using a Jenoptik ProgRes C5 colour digital camera (Jenoptik, Jena, Germany). DIC was used for high power observation to visualise unstained, or weakly stained, regions of tissue and provide additional context.

Results

The CS sulphation motif epitopes showed complex, dynamic and highly specific distributions that varied throughout development, growth and aging.

Embryonic day 15

At the E15 stage, prior to disc differentiation, the primitive vertebral column consisted of a repeating segmental arrangement of cartilaginous early vertebral body and cellular IVD condensation surrounding the embryonic notochord (Figs. 7-10). Immunoperoxidase labelling revealed differences in the expression of the distinct sulphation motif epitopes. The 3B3(-) epitope was not detected at E15 (Fig. 7), whereas the 4C3 (Fig. 8) and 7D4 (Fig. 9) epitopes were both detectable within the cellular IVD condensations, but not the vertebral bodies. In contrast, the 6C3 epitope was weakly identifiable only within the notochordal sheath (Fig. 10).

Embryonic day 17

At E17 the notochord had bulged intervertebrally giving rise to the nucleus pulposus, and the surrounding cellular disc condensations had differentiated into histologically distinct cartilaginous inner and fibroblastic outer annuli (Figs. 11-14a,b). Immunoperoxidase labelling showed that the 3B3(-) epitope was most prominent within the cartilage matrix of the inner annulus, extending laterally into the insertional region of outer annulus into vertebral bodies (i.e. future end-plate) and also within the perichondrium of the vertebral bodies (Figs. 11a,b). Labelling was also present in the notochordal sheath and between notochordal cells of the nucleus pulposus (Fig. 11a,b). The 4C3 (Figs. 12a,b) and 7D4 (Figs. 13a,b) epitopes had a similar tissue distribution to 3B3(-); however, both epitopes were also detectable within the vertebral bodies at this stage, having a cellular/pericellular localisation (Figs 12a,b and 13a,b respectively). Both epitopes were also intimately associated with the cells of the inner annulus as well as occurring within their surrounding cartilaginous ECM (Figs. 12a,b and 13a,b, respectively). In marked contrast, the 6C3 epitope was only identifiable within the cambial layer of the perichondrium at the ventral ends of lumbar vertebral bodies at this stage (Figs. 14a,b).

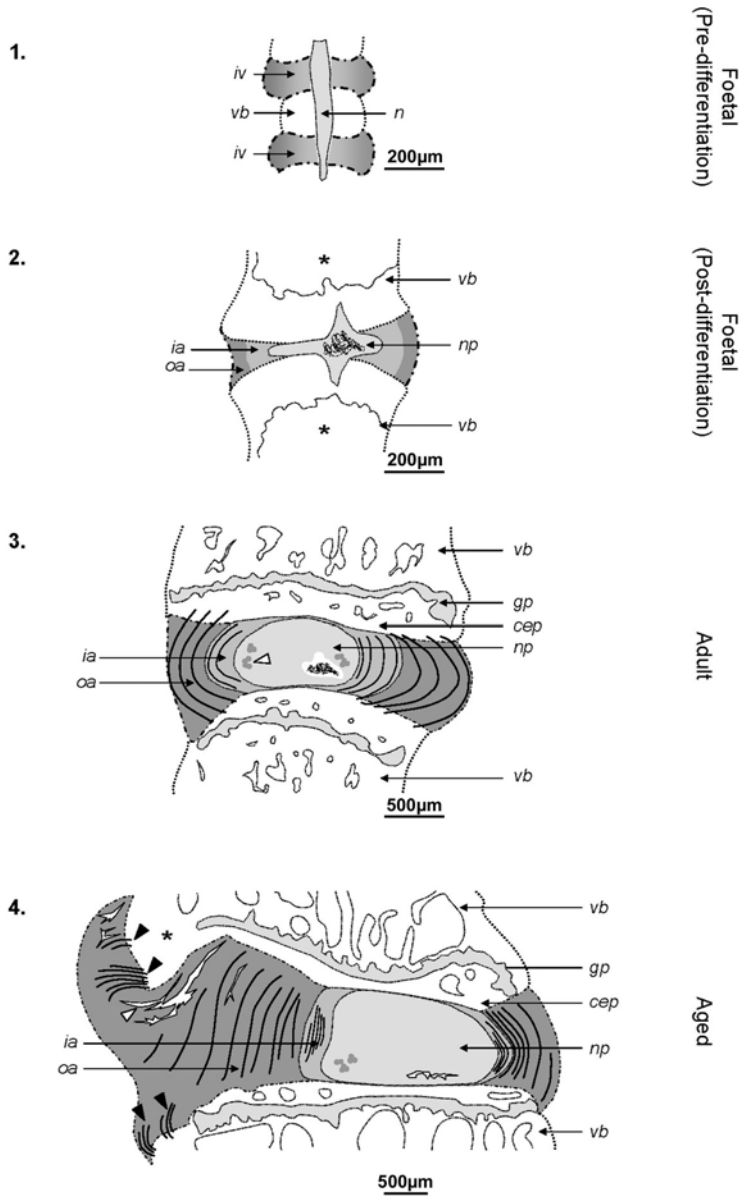

Plate 1: Schematics summarising stages in the development of the rat IVD. Fig. 1. IVD anlagen at embryonic day (E)15. At this stage the disc anlagen (iv) consist of regular dense condensations of mesenchyme that surround the notochord (n). Condensing cartilage of the developing vertebral bodies (vb) occurs between adjacent disc anlagen. **Fig. 2.** Late foetal disc. Between E15 and E16, the notochord bulges intervertebrally to form the nucleus pulposus (np). The disc condensations differentiate into the inner (ia) and outer (oa) annulus fibrosus. Prior to birth the vertebral bodies (vb) begin to undergo primary ossification (asterisk). **Fig. 3.** Adult, 4 month, disc. The annular lamellae are anchored within the cartilage endplates (cep) of the vertebral bodies (vb), which have undergone secondary ossification. The nucleus pulposus, in addition to notochordal cells, contains clusters of chondrocyte-like cells at its margins (white arrow-head) gp, growth plate. **Fig. 4.** Aged, 24 month, disc. The disc has a more disorganised morphology, tissue boundaries are indistinct and there are overt signs of degeneration including annular tears (white arrow-head), calcification and osteophytosis (asterisk). Black arrow-heads indicate insertional regions of outer annular lamellae into vertebral bodies.

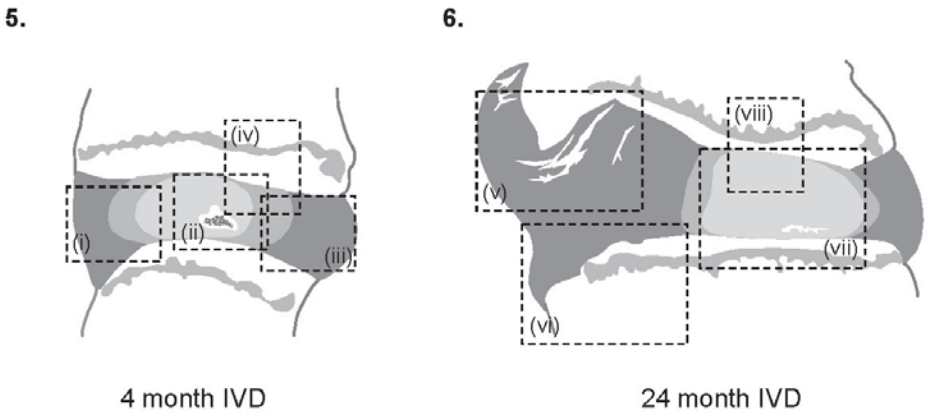

Plate 2: Schematics summarising the histological regions of disc studied in adult and aged specimens. Boxed areas demarcate the discal regions that were chosen for comparative analysis of CS sulphation patterns. **Fig. 5.** Adult (4 month) disc schematic. *Region (i)*: anterior annulus (depicted in Figures 23-26); *region (ii)*: nucleus pulposus (depicted in Figs. 27-20a,b); *region (iii)*: posterior annulus fibrosus (depicted in Figs. 31-34) and *region (iv)*: cartilage endplate/growth plate/vertebral body interface zones (depicted in Figs. 35-38a,b). **Fig. 6.** Aged (24 month) disc schematic. *Region (v)*: anterior annulus; superior aspect (depicted in Figs. 39-42a,b); *region (vi)*: anterior annulus fibrosus; inferior aspect (depicted in Figs. 43-46); *region (vii)*: nucleus pulposus (depicted in Figs. 47-50a,b) and *region (viii)*: cartilage endplate/growth plate/vertebral body interface zones (depicted in Figs. 51-54a,b).

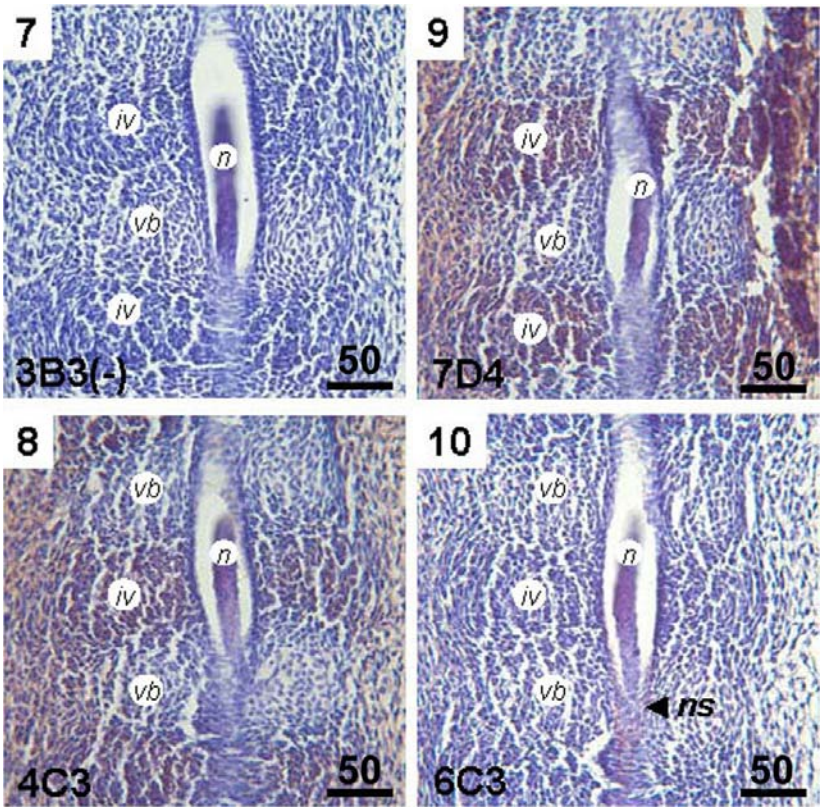

Plate 3. The distribution of CS sulphation motif epitopes within lumbar segments at embryonic day [E]15, prior to the onset of disc differentiation. Scale bars denoted in µm. Spinal axis runs rostrocaudally from top to bottom. At E15 the cellular IVD condensations (*iv*) have not yet undergone differentiation and the notochord (*n*) runs centrally through these and the vertebral bodies (*vb*). **Fig. 7-10** show immunostaining patterns for 3B3(-), 4C3, 6C3 and 7D4 respectively. 3B3(-) epitope is absent, 4C3 is localised to the disc condensations, 6C3 to notochordal sheath (arrow head) and 7D4 to the disc condensations.

Embryonic day 19

By E19, the labelling patterns of the CS sulphation motif antibodies had become more restricted in their tissue distributions (Figs. 15-18a,b). The 3B3(-) epitope remained prominent within the inner annulus, at the insertional region of outer annulus into vertebral bodies and also within the perichondrium, but labelling appeared reduced in the nucleus pulposus (Figs. 15a,b). There was a similar reduction of labelling in the nucleus pulposus with mAbs 4C3 and 7D4 (Figs. 16a,b and 17a,b, respectively). Furthermore, the cellular/pericellular labelling of the vertebral bodies, noted at E17, had diminished almost entirely; thus both epitopes remained at the interface regions between inner and outer annulus and outer annulus and vertebral bodies (Figs. 16a,b and 17a,b, respectively). The distribution of the 6C3 epitope, meanwhile, remained unchanged (Figs. 18a,b).

Embryonic day 21

Prior to birth, the disc had undergone further enlargement and the vertebral bodies had begun to ossify (Figs. 19-22a,b). The immunoperoxidase labelling patterns became further restricted with all four of the CS sulphation motif epitopes occurring within the inner annulus and nucleus pulposus (Figs. 19-22a,b). The labelling intensity was greatest with mAbs 3B3(-) and 7D4, particularly within the notochordal sheath (Figs. 19a,b and 21a,b, respectively), with weaker labelling with mAbs 4C3 and 6C3 (Figs. 20a,b and 22a,b, respectively). There was also very weak labelling of the cartilaginous ends of the vertebral bodies with mAbs 7D4 and 6C3 (Figs. 21a,b and 22a,b, respectively).

4 months

At 4 months the CS sulphation motif epitopes were widely distributed in the disc with distinct, but overlapping, distributions. Expression of the 3B3(-) epitope was restricted entirely to the discal tissues (Figs. 23, 27a,b and 31) and was absent from both the growth plate and cartilage end plate of the vertebral bodies (Figs. 35a,b). The ECM of the nucleus pulposus labelled prominently for 3B3(-); however the territorial matrix that surrounded chondrocyte clusters at the margins of the nucleus were devoid of this epitope (Fig. 27a); despite some cellular positivity (Fig. 27b). The extent of 3B3(-) immunolabelling in the annulus decreased towards its periphery (Figs. 23 & 31): within the inner annulus, labelling was mostly of the pericellular and inter-territorial matrix compartments; whereas in the outer annulus labelling was mainly pericellular (Figs. 23 and 31). The 4C3 epitope had a similar distribution in the disc (Figs. 24, 28a,b and 32) to 3B3(-) but was also weakly present in the growth plate (Figs. 36a,b). It was also strongly associated with some of the chondrocyte-like cells of the nucleus pulposus, but not their surrounding ECM (Fig. 28a,b). The 7D4 (Figs. 25, 29a,b, and 33) and 6C3 epitopes (Figs. 26, 30a,b and 34) had broadly similar distributions in the disc to 3B3(-) and 4C3; however, they were less noticeable within the pericellular matrix compartment of discal tissues. In the nucleus pulposus, 7D4 and 6C3 were also associated with the surface of the chondrocyte-like cells, but not their territorial ECM (Figs. 29a,b and 30a,b). These epitopes were also more prominent within the growth plate (Figs. 37a,b and 38a,b) than 3B3 (-) and 4C3 with matrix label associated with the prehypertrophic and upper hypertrophic zones.

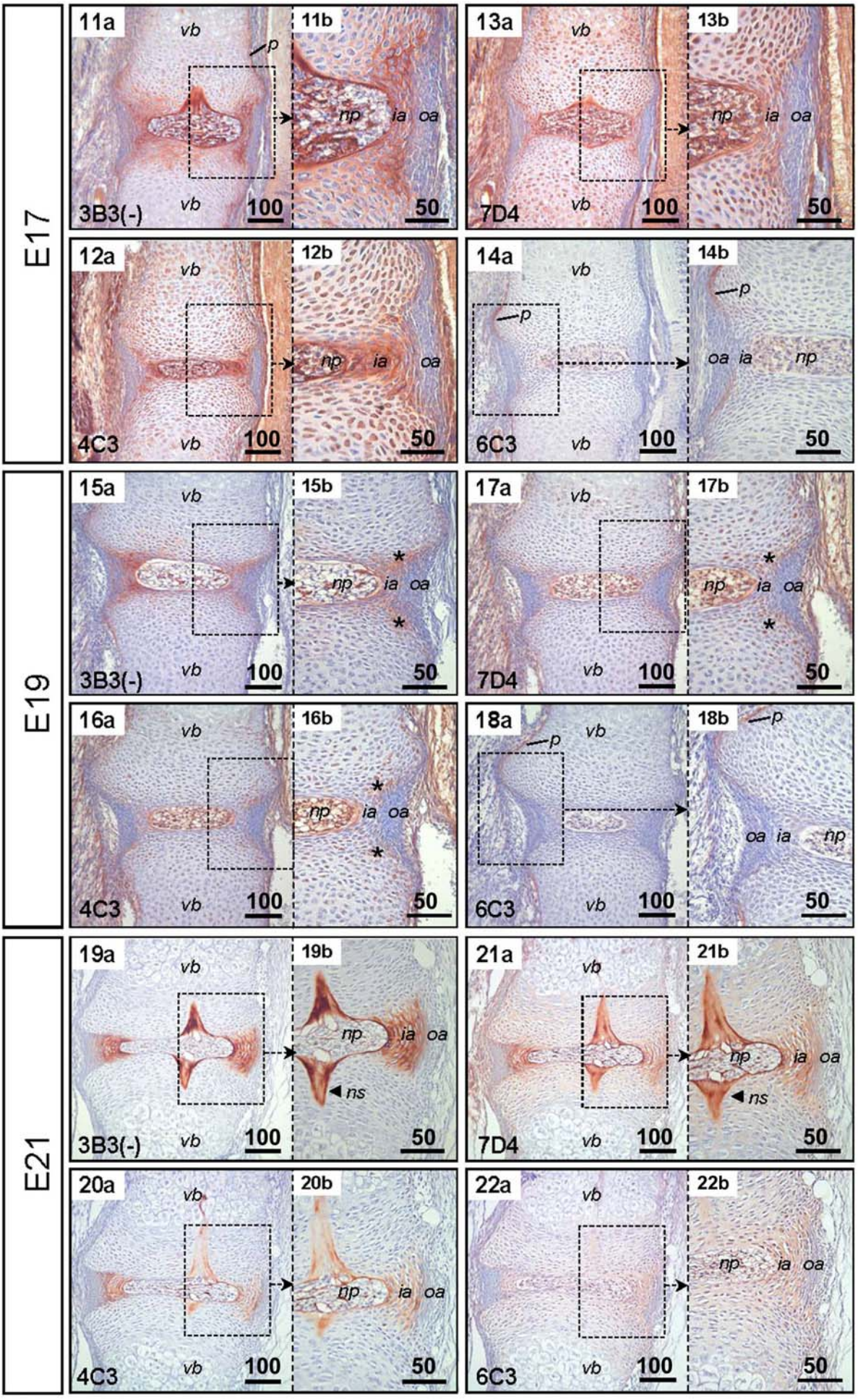
E17
11a
vb
p
11b
np
ia
oa
3B3(-)
vb
100
50
13a
vb
13b
np
ia
oa
7D4
vb
100
50
12a
vb
12b
np
ia
oa
4C3
vb
100
50
14a
vb
p
14b
p
oa
ia
np
6C3
vb
100
50
E19
15a
vb
15b
*
np
ia
oa
*
3B3(-)
vb
100
50
17a
vb
17b
*
np
ia
oa
*
7D4
vb
100
50
16a
vb
16b
*
np
ia
oa
*
4C3
vb
100
50
18a
p
vb
18b
p
oa
ia
np
6C3
vb
100
50
E21
19a
vb
19b
np
ia
oa
ns
3B3(-)
vb
100
50
21a
vb
21b
np
ia
oa
ns
7D4
vb
100
50
20a
vb
20b
np
ia
oa
4C3
vb
100
50
22a
vb
22b
np
ia
oa
6C3
vb
100
50

Plate 4. The distribution of CS sulphation motif epitopes in the disc and vertebral body during foetal development, post-disc differentiation. **Scale bars denoted in μm.** Spinal axis runs rostrocaudally from top to bottom. *np,* nucleus pulposus; *ia,* inner annulus *oa,* outer annulus; *p*, perichondrium; *ns*, notochordal sheath; *vb*, vertebral body. Low power images on the left (11-22a) are shown in detail in adjacent higher power images on the right (11-22b). ***Upper panel (Figs. 11-14a,b):*** CS labelling patterns at E17. **Figs. 11a, b.** Immunostaining pattern of 3B3(-) at E17. Note expression of 3B3(-) within the disc and at the ends of the vertebral bodies. **Figs. 12a, b.** Immunostaining pattern of 4C3 at E17. **Figs. 13a,b.** Immunostaining pattern of 7D4 at E17. Note cellular expression of the 4C3 and 7D4 epitopes within the vertebral bodies and both cell and ECM expression within the inner annulus. **Figs. 14a,b.** Immunostaining pattern of 6C3 at E17. Note expression of 6C3 epitope within the perichondrium (p) on the ventral aspect of the vertebral bodies. ***Middle panel (Figs. 15-18,b):*** **CS labelling patterns at E19**. **Figs. 15a,b.** Immunostaining pattern of 3B3(-) at E19. **Figs. 16a, b.** Immunostaining pattern of 4C3 at E19. **Fig. 17a,b.** Immunostaining pattern of 7D4 at E19. Note loss of cellular expression of the 4C3 and 7D4 epitopes within the vertebral bodies, and (with the exception of 6C3) the more restricted distribution of sulphation epitopes to inner/outer annulus and annulus/vertebral body tissue interfaces (*denoted by asterisks*). **Figs. 18a,b.** Immunostaining of 6C3 within the perichondrium (*p*) at E19. ***Bottom panel (Figs. 19-22a,b):*** **CS labelling patterns at E21**. **Figs. 19a,b.** Immunostaining pattern of 3B3(-) at E21. **Figs. 20a, b.** Immunostaining pattern of 4C3 at E21. **Figs. 21a,b.** Immunostaining pattern of 6C3 at E21. **Figs. 22a,b.** Immunostaining pattern of 7D4 at E21. Note CS sulphation motifs are localised within the inner annulus and notochordal sheath

24 months

At 24 months, all four epitopes were identifiable throughout the disc. In the annulus they occurred within the ECM between adjacent collagenous lamellae, particularly within the pericellular matrix (Figs. 39-42a,b). More diffuse and prominent ECM labelling occurred where the outer annular lamellae inserted directly into the vertebral bodies i.e., the annular attachment zones (Figs. 39-42a,b and 43-46). They were also associated with clusters of cells bordering overt tears in the outer annulus (Fig. 39-42a,b). Within the nucleus pulposus, all four CS sulphation motif epitopes were represented (Figs. 47-50a,b): the 3B3(-) and 7D4 epitopes (Fig. 47a,b and 49a,b respectively) were distributed more broadly than 4C3, which was absent from the pericellular matrix (Fig. 48a,b), and 6C3, which was only weakly present in the ECM, but had a strong cellular association (Fig. 50a,b). In the growth plate, the columnar and zonal structure had broken down, leading to the formation of chondrocyte clusters which labelled only weakly with 4C3 and 6C3 (Fig. 52a,b and 54a,b respectively). In contrast, the 7D4 epitope was prominent throughout the growth plate matrix (Fig. 53a,b) and 3B3(-) was restricted specifically to the capsular matrix surrounding the chondrocyte clusters (Fig. 51a).

Discussion

Different CS sulphation motif epitopes occur in a wide range of embryonic musculoskeletal tissues, including bone, muscle, articular cartilage, growth plate, and at sites of epithelial-mesenchymal interaction, such as skin, tooth, gut, and lung (Sorrel *et al*., 1988; Sorrel and Caterson, 1989; Sorrel *et al*., 1990; Sorrel *et al*., 1996; Caterson *et al*., 1990; Mark *et al*., 1990; Visco *et al*., 1993; Gibson *et al*., 1996; Hayes *et al*., 2008). In the spine, we have previously described some aspects of the distribution of the 3B3(-) and 7D4 epitopes in a series of foetal rat IVDs (Hayes *et al*., 2001), showing that distributions coincide with key tissue interfaces and growth zones both within the disc and between the disc and vertebral bodies. In a study of cartilage histomorphogenesis in the rat spine, Mark *et al*. (1989) described the distribution of a CS epitope, using mAb MC21C, occurring within 6-sulphated segments of intact CS chains. Other studies have shown that the 3B3(-) and 7D4 epitopes are associated with disc degeneration and possible cellular reparative processes (Roberts *et al*., 1994; Inkinen *et al*., 1998; Melrose *et al*., 2000). The results of this study add significantly to the above data and it is the first, to our knowledge, to describe patterns of differential CS sulphation during intervertebral disc development, growth and aging

The major morphological event in rat disc developmental occurs between E15 and E17, coincident with the initial disc differentiation stage (Rufai *et al*., 1995), and closely parallels that occurring in the 55 day human foetus (Peacock, 1951a). The presence of CS motifs recognised by 4C3 and 7D4 in the disc anlagen and not the vertebral body anlagen contrasts strikingly with distributions of the 'normal' C-4-S and C-6-S stub epitopes, which are in the vertebral body and not the disc anlagen, mostly in association with aggrecan (Rufai *et al*., 1995; Hayes *et al*., 2001). There could be a number of functional reasons for these distributions. There could be a different set of regulatory molecules (e.g., growth factors, cytokines, morphogens, chemokines or enzymes) associated with the different GAG populations, leading to different populations of regulatory molecules associated with the various tissue differentiation pathways. For example, during murine axial morphogenesis the expression patterns of TGF-β isoforms, particularly TGF-β3 (Pelton, 1990; Schmid *et al*., 1991), display many similarities with some of the labelling patterns of the CS sulphation epitopes seen here; suggestive of potential co-associations. Thus the embryo may 'pre-programme' the ECM to enable the dramatic changes that are about to occur in notochordal bulging and the establishment of spinal structure. There could also be other reasons: sulphated GAGs attract water more strongly than non-sulphated forms and the water holding capacity of PGs is proportional to the density of carboxyl and sulphate

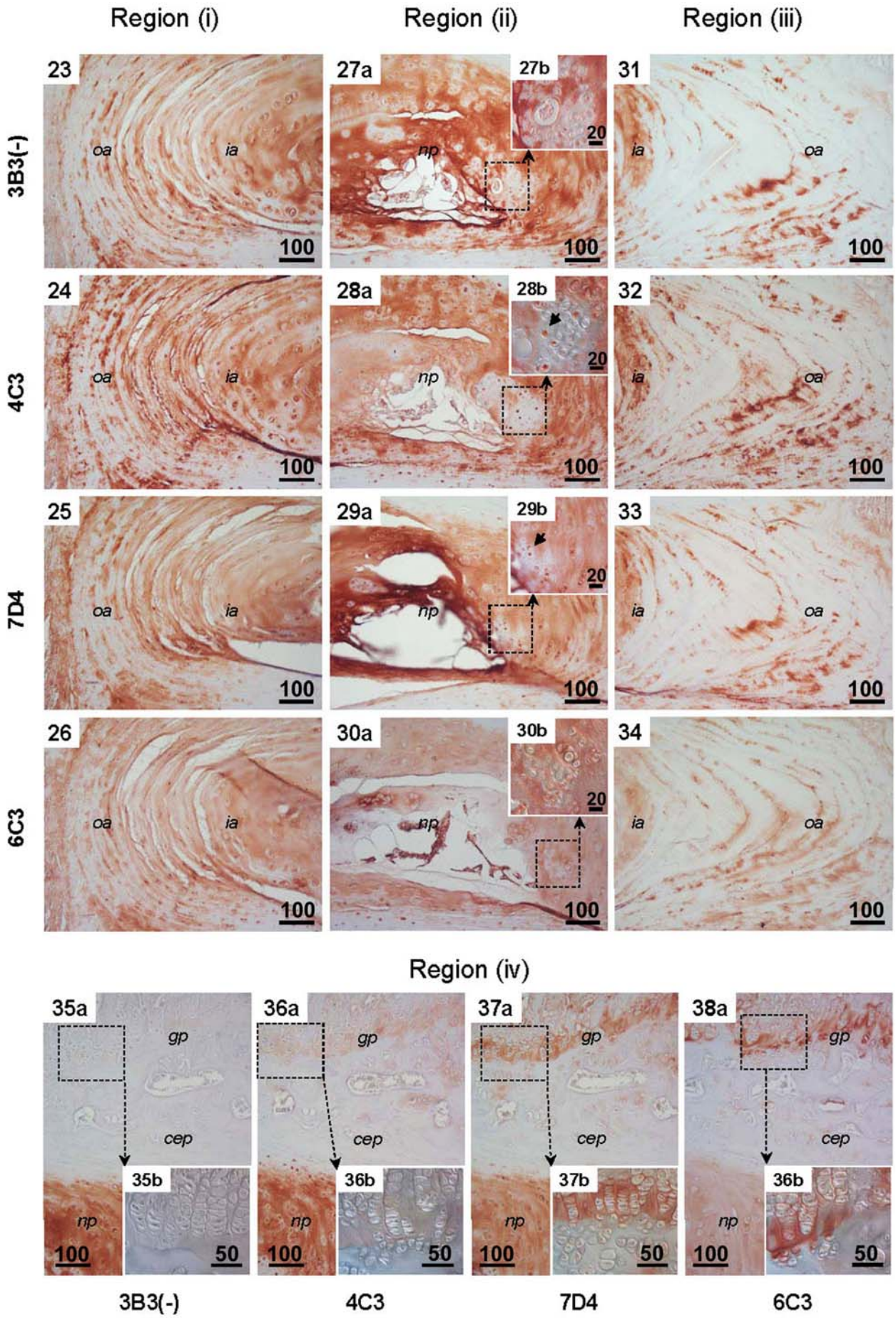
Region (i)
Region (ii)
Region (iii)
3B3(-)
4C3
7D4
6C3
23
27a
27b
31
24
28a
28b
32
25
29a
29b
33
26
30a
30b
34
oa
ia
np
20
100
Region (iv)
35a
36a
37a
38a
gp
cep
35b
36b
37b
50
3B3(-)
4C3
7D4
6C3

Plate 5. The distribution of CS sulphation motif epitopes in the adult (4month) lumbar rat disc/vertebral body. Scale bars denoted in μm. Spinal axis runs rostrocaudally from top to bottom. ***Region (i)*:** anterior annulus (Figs. 23-26); ***Region (ii)*:** nucleus pulposus (Figs. 27-30a,b; boxed areas show detail (*inset*) of labelling associated with chondrocyte clusters); ***Region (iii)*:** posterior annulus fibrosus (Figs. 31-34) and ***Region (iv)*:** cartilage endplate/growth plate/vertebral body interface zones (Figs. 35-38a,b; boxed areas show detail (*inset*) of growth plate labelling). *cep*, cartilage endplate; *gp*, growth plate; *ia*, inner annulus; *oa*, outer annulus; *np*, nucleus pulposus. **Figs. 23, 27a,b, 31, and 35a,b.** Immunostaining pattern of 3B3(-) at 4 months. **Figs. 24, 28a,b, 32, and 36a,b.** Immunostaining pattern of 4C3 at 4 months. **Figs. 25, 29a,b, 33, and 37a,b.** Immunostaining pattern of 7D4 at 4 months. **Figs. 26, 30a,b, 34, and 38a,b.** Immunostaining of 6C3 at 4 months. Note widespread labelling of all four CS sulphation motifs throughout the disc at this stage.

radicals of their side chains (Urban and Maroudas, 1980; Bogduk, 2005). As the cartilage of the vertebral bodies differentiate, aggrecan rich in 4- and 6- sulphated CS chains is produced in large quantities, the GAGs imbibe water and, constrained by type II collagen exert a swelling pressure inwards on the notochord. This appears to drive its segmental dilation into the IVD condensations (Rufai *et al.*, 1995; Aszodi *et al*., 1998). Perhaps the presence of the CS sulphation variants and absence of C-4-S and C-6-S stubs in the disc anlagen at this stage are associated with reduced swelling pressure compared to the vertebral bodies and allows the bulging of the notochord to occur in these "weak" points between the vertebral bodies.

After notochordal bulging and annulus differentiation, the CS motifs are associated with the cartilaginous components of the foetal spine (inner annulus, vertebral body). They show significant temporal and spatial distributional changes in the foetal ages studied. It is clear that in development, despite their histological similarity, the cartilages of the vertebral body and intervertebral disc, are substantially different in their populations of CS sulphation motifs. Label may be just in the matrix (3B3[-]) or be cell and matrix associated (4C3, 7D4), as well as being very dynamic in its expression pattern; for example, with the latter, labelling may change in a short developmental period from being purely cellular to being purely matrix-associated. However, labelling does not appear in the fibrous outer annulus until late in development and during growth. This may relate to the fact that fibrocartilage differentiates from the foetal fibrous outer annulus some time after its initial development, probably relating to increased compressive load transferred from the nucleus pulposus with the onset of movement (Rufai *et al*., 1995; Hayes *et al*., 2001).

The dramatic changes that occur in the specific expression patterns of CS sulphation motifs during foetal development, strongly suggests that they occur on a range of different PGs, both matrix and cell-associated. Furthermore, it indicates that the cells differentially modify the composition of their GAG chains on their PGs (via differential regulation of their sulfotransferase enzymes) in a highly specific, spatially distinct manner. The biological purpose of these CS modifications are, as yet, unclear and are the subject of current enquiry; but clearly must have functional significance because CS sulphation is an energy consuming process (Bowman and Bertozzi, 1999). Thus, until the precise structure and function of the distinct CS sulphation epitopes are known and the identity of the PGs on which the epitopes reside are established the functional significance of these distributions cannot be fully resolved and remains a matter of conjecture.

Cellular localisation could indicate intracellular synthesis and processing, localisation to the plasmalemmal or pericellular PGs, and/or internalisation of such PGs (Dziewiatowski, 1962; Thorp and Dorfman, 1963; Campbell and Schwartz, 1988). Association of label with cell surface PGs could have implications for control of differentiation and morphogenesis of the cartilaginous components of disc and vertebra. Perlecan can have CS chains substituted on its core protein, thus could act as a host for the various sulphation motifs, and occurs pericellularly in the foetal vertebral body (Melrose *et al*., 2003, 2008). Perlecan has a well established role in binding FGF in the growth plate (Smith *et al*., 2007; see below), and thus might also play important regulatory roles in early developmental processes occurring within the spine. The syndecan family of trans-membrane PGs (Couchman, 2010) also have CS chains, and syndecan-3 is a direct regulator of chondrocyte proliferation in endochondral ossification (Shimazu *et al*., 1996; Kosher *et al*., 1998; Kirsch *et al*., 2002; Shimo *et al*., 2010) and, similarly therefore, could be involved in regulating the proliferative phase of chondrogenesis within the developing vertebral bodies.

In the ECM, the CS motifs must be associated with CS chains on matrix PGs. Here, the prime candidate is aggrecan, simply because of its abundance in cartilage, and the abundance of CS side chains on its core protein (Watanabe *et al*., 1998). Versican is also a possibility, it being present in cartilage of the early vertebral body, inner annulus and the fibrous outer annulus (Hayes *et al*., 2001), and playing an important role in regulating on the onset of chondrogenesis (Kamiya *et al*., 2006). Furthermore, the small leucine rich PGs (SLRPS) decorin and biglycan have reported roles in collagen fibrillogenesis and growth factor binding in the annulus (Götz *et al*., 1997), and so some of our labelling patterns may also be associated with these. In older discs, and in degenerative disease, 3B3(-) and 7D4 epitopes appear to occur within the CS chains of a range of cell-associated and matrix PGs including decorin, biglycan and versican (Roberts *et al*., 1994; Inkinen *et al*., 1998; Melrose *et al*., 2000).

The similarity seen in the labelling patterns of 3B3(-), 4C3 and 7D4 at E19 confirms and also expands some previous observations (Mark *et al*., 1989; Hayes *et al*., 2001). The presence of these epitopes in the inner annulus

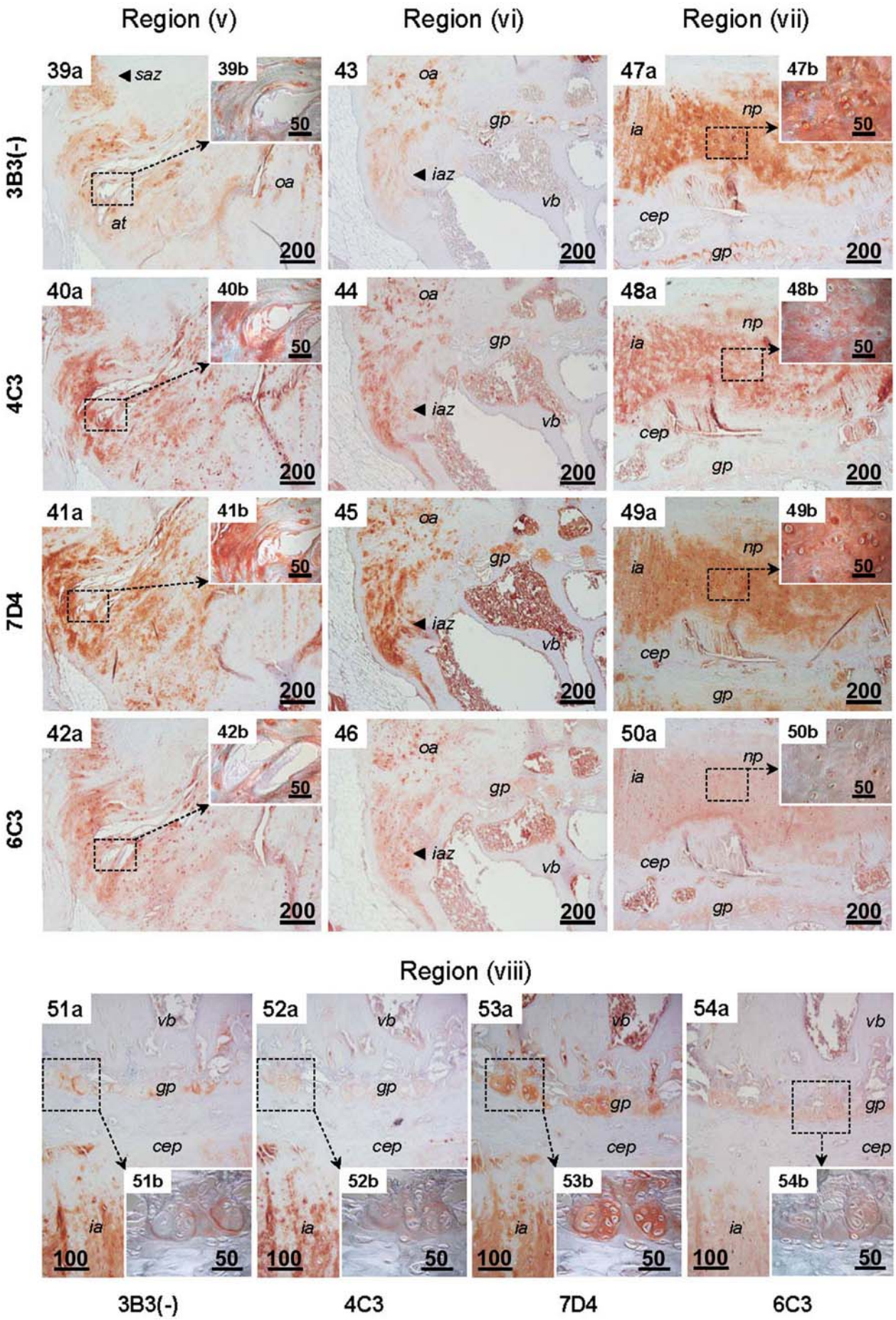
Region (v)
Region (vi)
Region (vii)
3B3(-)
4C3
7D4
6C3
39a
saz
39b
50
oa
at
200
43
oa
gp
iaz
vb
200
47a
47b
np
ia
50
cep
gp
200
40a
40b
50
200
44
oa
gp
iaz
vb
200
48a
48b
np
ia
50
cep
gp
200
41a
41b
50
200
45
oa
gp
iaz
vb
200
49a
49b
np
ia
50
cep
gp
200
42a
42b
50
200
46
oa
gp
iaz
vb
200
50a
50b
np
ia
50
cep
gp
200
Region (viii)
51a
vb
gp
cep
51b
ia
100
50
52a
vb
gp
cep
52b
ia
100
50
53a
vb
gp
cep
53b
ia
100
50
54a
vb
gp
cep
54b
ia
100
50
3B3(-)
4C3
7D4
6C3

Plate 6. The distribution of CS sulphation motif epitopes in the aged (24month) lumbar rat disc/vertebral body. Scale bars denoted in μm. Spinal axis runs rostrocaudally from top to bottom. ***Region (v)*:** anterior annulus; superior aspect (Figs. 39-42a,b; boxed areas show detail (inset) of labelling around annular tears; ***Region (vi)*:** anterior annulus fibrosus; inferior aspect (Figs. 43-46); ***Region (vii)*:** nucleus pulposus (Figs. 47-50a,b) and ***Region (viii)*:** cartilage endplate/growth plate/vertebral body interface zones (Figs. 51-54a,b; boxed areas show detail (inset) of growth plate labelling). *at*, annular tear; *cep*, cartilage endplate; *gp*, growth plate; *ia*, inner annulus; *iaz*; inferior attachment zone; *oa*, outer annulus; *np*, nucleus pulposus; *saz*, superior attachment zone. **Figs. 39a,b, 43, 47a,b, and 51a,b.** Immunostaining pattern of 3B3(-) at 24 months. **Figs. 40a,b, 44, 48a,b, and 52a,b.** Immunostaining pattern of 4C3 at 24 months. **Figs. 41a,b, 45, 49a,b, and 53a,b.** Immunostaining pattern of 7D4 at 24 months. **Figs. 42a,b, 46, 50a,b, and 54,b.** Immunostaining of 6C3 at 24 months. Note prominent labelling of all four CS sulphation motifs at sites of annular attachment; surrounding annular tears; and within the nucleus pulposus and growth plate.

and their outward extension, along the insertional region between outer annulus fibrosus and vertebral bodies, into the perichondrium of the vertebral bodies implies significant roles in differentiation and behaviour of these highly specialised tissues. This region is little studied but is crucial to spine function, as the annulus must be solidly attached to the vertebral bodies for the normal range of spinal motion. This region can be regarded as analogous to the fibrocartilaginous enthesis, or attachment zone, of tendons and ligaments (Benjamin and Ralphs, 1999) and these sites label for the CS sulphation epitopes during postnatal growth and aging, similar to enthesis (Milz *et al*., 2006). The function of the distinctive GAG populations at these sites is unclear, but could be associated with specific PGs, and/or be associated with growth factor binding or sequestration relating to tissue differentiation or metaplasia. Their association with the innermost regions of the outer annulus is of potential significance as these regions are the first of the outer annulus to differentiate into fibrocartilage as the animal grows (Rufai *et al*., 1995; Hayes *et al*., 2001). The restricted distribution of 6C3 to the ventral aspect of the perichondrium at the bulging ends of the vertebral bodies at early stages may be related to vertebral growth. The label appears to be associated with the cambial layer of the perichondrium, which generates new chondrocytes for appositional growth (Kronenberg, 2007), and vertebral bodies are clearly expanding outwards in these regions. Interestingly there is no such label posteriorly, suggesting that growth may be slower towards the spinal cord. The vertebral body may thus be growing thicker but without impinging on the developing vertebral canal.

Postnatally the disc tissues become more uniform in CS sulphation motif epitope expression. Distributions appear to depend on the extent of cartilaginous differentiation in the different discal tissues – thus at 4 months the cartilage of the inner annulus has uniform matrix label, whereas the differentiating fibrocartilage of the outer annulus has pericellular label across its width extending to its attachment with the endplate. At 24 months, presumably with fully differentiated fibrocartilage, the outer annulus shows more widespread matrix label. The nucleus pulposus, cartilaginous in these sections, also labels for all of the CS epitopes. Notably, we do not observe a notochordal remnant at 24 months, although notochordal remnants do occur in rat discs of this age (Rufai *et al*., 1995), suggesting that it has not been sampled in the sections used here. Surprisingly, the only cartilaginous tissue showing little evidence of labelling is the cartilage endplate. The labelling pattern of the growth plate, in contrast, is complex, with matrix label associated with the stacks of flattened chondrocytes of pre-hypertrophic and upper hypertrophic zones in 4 month animals. Recent evidence indicates that correct sulphation of CS on growth plate PGs is essential for proper Indian Hedgehog (Ihh) signalling and normal bone growth (Cortes *et al*., 2009). Undersulphation of CS PGs results in reduced chondrocyte proliferation and bone shortening through altered Ihh signalling (Gualeni *et al*., 2010). The abundance of perlecan in growth plate cartilage and its known role in growth plate function, in mediating binding and delivery of FGF-2 to FGF receptors via CS and heparan (Smith *et al*., 2007), raises the possibility that this PG may host the CS sulphation motifs studied here. In 24 month animals the growth plate is present but its columnar and zonal structure has broken down, leading to the formation of chondrocyte clusters which also label for most of the sulphation epitopes.

The presence of chondrocyte-like clusters at the margins of the nucleus pulposus of the rat disc at 12 months have been described previously (Rufai *et al*., 1995) and are a normal feature of its aging. Recent data (reviewed by Risbud *et al*., 2010) indicates that they are derived from notochordal cells of the anlagen disc, which are also present within the nucleus at this stage. Our study shows that both cell phenotypes synthesize the different CS sulphation motifs; however, the latter appear more prolific in this regard. Only a small proportion of the chondrocyte-like cells within individual clusters express the different CS motifs, reflecting the metabolic heterogeneity of these cells. The noted absence of CS motifs within the capsular ECM that surrounds the chondrocyte-like cells also suggests that they do not contribute their CS moieties to the bulk load-bearing matrix of the nucleus pulposus, as their notochordal precursors appear to do throughout development. Previous studies of chondrocyte clusters in the nucleus pulposus of degenerating discs have shown that they are highly proliferative (Johnson *et al*., 2001), and are positive for a range of connective tissue growth factors, including members of the TGF-β, FGF and PDGF families (Tolonen *et al*., 2006). It is feasible, therefore, that the CS motifs on these cells may contribute to growth factor sequestration or binding and thus control local cellular proliferation / differentiation events within the nucleus.

Taken together, the dynamics of the CS motif distributions in early stages; their occurrence in growth plates and broad distribution in aged animals, suggests roles in the control of tissue development and differentiation. Subsequently, they may be involved in mature tissue function and homeostasis. In summary, this study expands significantly upon our previous findings (Hayes *et al*., 2001) and, coupled with the emerging knowledge of new protein-GAG interactions from glycomics, underscores the importance of novel sulphation of CS PGs in the differentiation, growth and aging of complex musculoskeletal connective tissues such as IVD.

Acknowledgements

Thanks to Mr Marc Isaacs for his assistance in photo-documenting the immunohistochemical labelling patterns in the rat intervertebral disc developmental series. This research was supported by funds from Arthritis Research UK (#18331).

References

Alliston T (2010) Chondroitin sulphate and growth factor signalling in the skeleton: possible links to MPS VI. J Pediatr Rehabil Med **3**: 129-138.

Aszodi A, Chan D, Hunziker E, Bateman JF, Fässler, R (1988) Collagen II is essential for the removal of the notochord and the formation of intervertebral discs. J Cell Biol **143**: 1399-1412.

Benjamin M, Ralphs JR (1999) The tendon/ligament-bone junction. In "Biology of the Synovial Joint" (Archer CW, Benjamin M, Caterson B Ralphs JR, eds) Harwood Academic Publishers, Taylor and Francis, Abingdon, UK, pp 361-373.

Bogduk N (2005) Clinical anatomy of the lumbar spine and sacrum. 4th ed. Churchill Livingstone, London.

Bowman K, Bertozzi CB (1999) Carbohydrate sulfotransferases: mediators of extracellular communication. Chem Biol **6**: 9-22.

Campbell SC, Schwartz NB (1988) Kinetics of intracellular processing of chondroitin sulphate proteoglycan core protein and other matrix components. J Cell Biol **106**: 2191-2202.

Caterson B, Mahmoodian F, Sorrell JM, Hardingham TE, Bayliss MT, Carney SL, Ratcliffe A, Muir H (1990) Modulation of native chondroitin sulphate structure in tissue development and in disease. J Cell Sci **97**: 411-417.

Cortes M., Baria AT, Schwartz NB (2009) Sulfation of chondroitin sulphate proteoglycans is necessary for proper Indian hedgehog signalling in the developing growth plate. Development **136**: 1697-1706.

Couchman JR (2010) Transmembrane signalling proteoglycans. Ann Rev Cell Dev Biol, in press.

Deepa SS, Umehara Y, Higashiyama S, Itoh Nand Sugahara K (2002) Specific molecular interactions of oversulfated chondroitin sulphate E with various heparin-binding growth factors. Implications as a physiological binding partner in the brain and other tissues. J Biol Chem **277**: 43707-43716.

Dziewiatkowski, D.D (1962) Intracellular synthesis of chondroitin sulphate. Cell Biol **13**: 359-364.

Gandhi NS, Mancera RL (2008) The structure of glycosaminoglycans and their interactions with proteins. Chem Biol Drug Des **72**: 455-482.

Gibson G, Lin DL, Caterson B, Foster B (1996) Type X collagen is colocalised with a proteoglycan epitope to form distinct morphological structures in bovine growth cartilage. Bone **19**: 307-315.

Götz W, Barnert S, Bertagnoli R Miosge N, Kresse H, Herken R (1997) Immunohistochemical localisation of the small proteoglycans decorin and biglycan in human intervertebral discs. Cell Tissue Res **289**: 185-190.

Gualeni B, Facchini M, De Leonardis F, Tenni R, Cetta G, Viola M, Passi A, Superti-Furga A, Forlino A, Rossi A (2010) Defective proteoglycan sulfation of the growth plate zones causes reduced chondrocyte proliferation via an altered Indian hedgehog signalling. Matrix Biol, in press.

Handel TM, Johnson Z, Crown SE, Lau ES, Sweeney M, Proudfoot AE (2005) Regulation of protein function by glycosaminoglycans – as exemplified by chemokines. Annu Rev Biochem **74**: 385-410.

Hardingham T (1994) The sulphation pattern in chondroitin sulphate chains investigated by chondroitinase ABC and ACII digestion and reactivity with monoclonal antibodies. Carbohydrate Res **255**: 241-254.

Hayes AJ Benjamin JR Ralphs JR. (2001) Extracellular matrix in development of the intervertebral disc. Matrix Biol **20**: 107-121.

Hayes AJ, Tudor D, Nowell MA, Caterson B and Hughes CE (2008) Chondroitin sulphate sulfation motifs as putative biomarkers for isolation of articular cartilage progenitor cells. J Histochem Cytochem **56**: 125-138.

Inkinen RI, Lammi MJ, Lehmonen S, Puustjärvi K, Kääpä E and Tammi MI (1998) Relative increase of biglycan and decorin and altered chondroitin sulphate epitopes in the degenerating human intervertebral disc. J Rheumatol **25**: 506-514.

Johnson WEB, Eisenstein SM, Roberts S (2001) Cell cluster formation in degenerate lumbar intervertebral discs is associated with increased cell proliferation. Conn Tiss Res **42**:197-207.

Kamiya N, Watanabe H, Habuchi H, Takagi H, Shinomura T, Shimizu K, Kimata K (2006) Versican/PG-M regulates chondrogenesis as an extracellular matrix molecule crucial for mesenchymal condensation. J Biol Chem **281**: 2390-2400.

Kawashima H, Atarashi K, Hirose M, Hirose J, Yamada S, Sugahara K, and Miyasaka M (2002) Oversulfated chondroitin/dermatan sulfates containing GlcAβ1/IdoAα1-3GalNAc(4,6-O-disulfate) interact with L- and P-selectin and chemokines. J Biol Chem **277**: 12921-12930.

Kirsch T, Koyama E, Liu M, Golub EE, Pacifici M (2002) Syndecan-3 is a selective regulator of chondrocyte proliferation. J Biol Chem **277**: 42171-42177.

Klüppel M, Wight TN, Chan C, Hinek A, Wrana JL (2005) Maintenance of chondroitin sulphation balance by

chondroitin-4-sulfotransferase 1 is required for chondrocyte development and growth factor signalling during cartilage morphogenesis. Development **132**: 3989-4003.

Kosher RA (1998) Syndecan-3 in limb skeletal development. Microsc Res. Techn **43**: 123-130.

Kronenberg HM (2007) The role of the perichondrium in fetal bone development. Ann NY Acad Sci **1116**: 59-64.

Mark MP, Butler WT, Ruch JV (1989) Transient expression of a chondroitin sulfate-related epitope during cartilage histomorphogenesis in the axial skeleton of fetal rats. Dev Biol **133**: 475-488.

Mark MP, Baker JR, Kimata K, Ruch JV (1990) Regulated changes in chondroitin sulfation during embryogenesis: an immunohistochemical approach. Int J Dev Biol **24**: 191-204.

Melrose J, Smith S, Ghosh P (2000) Differential expression of proteoglycan epitopes by ovine intervertebral disc cells. J Anat **197**: 189-198.

Melrose J, Smith S, Ghosh P, Whitelock J (2003) Perlecan, the multidomain heparin sulphate proteoglycan of basement membranes, is also a prominent components of the cartilaginous primordial in the developing human foetal spine. J Histochem Cytochem **51**:1331-1341.

Melrose J, Hayes AJ, Whitelock JM, Little CB (2008) Perlecan, the "jack of all trades" proteoglycan of cartilaginous weight-bearing connective tissues. Bioessays **30**: 457-469.

Merry CLR, Astrautsove SA (2008) Glycans in evolution and development. Workshop on glycoscience and development. EMBO Rep **9**: 716-622.

Milz S, Aktas T, Putz R Benjamin M (2006) Expression of extracellular matrix molecules typical of articular cartilage in the human scapholunate interosseous ligament. J Anat **208**: 671-679.

Nandini CD, Mikami T, Ohta M, Itoh N, Akiyama-Nambu F Sugahara K (2004) Structural and functional characterization of oversulfated chondroitin sulfate/dermatan sulfate hybrid chains from the notochord of hagfish. Neuritogenic and binding activities for growth factors and neurotrophic factors. J Biol Chem **279**: 50799-50809.

Peacock A (1951a) Observations on the pre-natal development of the intervertebral disc in man. J Anat **85**: 260-274.

Peacock A (1951b) Observations on the post-natal structure of the intervertebral disc in man. J Anat **86**: 162-179.

Pelton RW, Dickinson ME, Moses HL, Hogan BLM (1990) In situ hybridisation analysis of TGFβ3 RNA expression during mouse development: comparative studies with TGFβ1 and β2. Development. **110**: 609-620.

Raman R, Sasisekharan V, Sassisekharan R (2005) Structural insights into biological roles of protein-glycosaminoglycan interactions. Chem Biol **12**: 267-277.

Risbud MV, Schaer TP, Shapiro IM (2010) Toward an understanding of the role of notochordal cells in the adult intervertebral disc: from discord to accord. Dev Dyn **239**: 2141-2148.

Roberts S, Caterson B, Evans H, Eisenstein SM (1994) Proteoglycan components of the intervertebral disc and cartilage endplate: an immunolocalisation study of animal and human tissues. Histochem J **26**: 402-411.

Rufai A, Benjamin M, Ralphs JR (1995) The development of fibrocartilage in the rat intervertebral disc. Anat Embryol **192**: 53-62.

Sasisekharen R, Raman R, Prabhakar V (2006) Glycomics approach to structure-function relationships of glycosaminoglycans. Annu Rev Biomed Eng **8**: 181-231.

Schmid P, Cox D, Bilbe, G, Maier R, McMaster GK (1991) Differential expression of TGFβ1, β2 and β3 genes during mouse embryogenesis. Development. **111**: 117-130.

Sharp CA, Roberts S, Evans H, Brown SJ (2009) Disc cell clusters in pathological human intervertebral discs are associated with increased stress protein immunolabelling. Eur Spine J **18**: 1587-1594.

Shimazu A, Nah HD, Kirsch T, Koyama E, Leatherman JL, Golden EB, Kosher RA Pacifici M (1996) Syndecan-3 and the control of chondrocyte proliferation during endochondral ossification. Exp Cell Res **229**: 126-136.

Shimo T, Gentili C, Iwamoto M, Wu C, Koyama E, Pacifici M (2004) Indian hedgehog and syndecan-3 coregulate chondrocyte proliferation and function during chick limb skeletogenesis. Dev Dyn **229**: 607-617.

Smith SM, West LA, Govindraj P, Zhang X, Ornitz DM, Hassell JR (2007) Heparan and chondroitin sulphate on growth plate perlecan mediate binding and delivery of FGF-2 to FGF receptors. Matrix Biol **26**: 175-184.

Sorrell JM, Caterson B (1989) Detection of age-related changes in the distribution of keratan sulfates and chondroitin sulfates in developing chick limbs: an immunocytochemical study. Development **106**: 657-663.

Sorrell JM, Lintala AM, Mahmoodian F, Caterson B (1988) Epitope-specific changes in chondroitin sulphate/dermatan sulphate proteoglycans as markers in the lymphopoietic and granulopoietic compartments of developing bursae of Fabricius. J Immunol **140**: 4263-4270.

Sorrell JM, Mahmoodian F, Schafer IA, Davis B Caterson B (1990) Identification of monoclonal antibodies that recognize novel epitopes in native chondroitin/dermatan sulphate glycosaminoglycan chains: their use in mapping functionally distinct domains of human skin. J Histochem Cytochem **38**: 393-402.

Sorrell JM, Carrino DA, Caplan AI (1996) Regulated expression of chondroitin sulfates at sites of epithelial-mesenchymal interaction: spatio-temporal patterning identified with anti-chondroitin sulphate monoclonal antibodies. Int J Devel Neurosci **14**: 233-248.

Thorp FK, Dorfman A (1963) The occurrence of intracellular chondroitin sulphate. J Cell Biol **18**: 13-17.

Tiedemann K, Olander B, Eklund E, Todorova L, Bengtsson M, Maccarana M, Westergren-Thorsson G, Malmström A (2005) Regulation of the chondroitin/dermatan fine structure by transforming growth factor-β1 through effects on polymer-modifying enzymes. Glycobiology **15**: 1277-1285.

Tolonen J, Grönblad M, Vanharanta H, Virri J, Guyer RD, Rytömaa T, Karaharju EO (2006) Growth factor

expression in degenerated intervertebral disc tissue. An immunohistochemical analysis of transforming growth factor beta, fibroblast growth factor and platelet-derived growth factor. Eur Spine J **15**: 588-596.

Urban J. Maroudas A (1980) The chemistry of the intervertebral disc in relation to its physiological function. Clin Rheum Dis **6**: 51-76.

Visco DM, Johnstone B, Hill MA, Jolly GA, Caterson B (1993) Immunohistochemical analysis of 3-B-3(-) and 7-D-4 epitope expression in canine osteoarthritis. Arthritis Rheum **36**: 1718-1725.

Walmsley R (1953) The development and growth of the intervertebral disc. Edinburgh Med J **60**: 341-364.

Watanabe H, Yamada Y, Kimata K (1998) Roles of aggrecan, a large chondroitin sulphate proteoglycan, in cartilage structure and function. J Biochem **124**: 687-693.

Editor's Note: All questions/comments from the reviewers of this paper were answered by text changes. Hence, there is no "Discussion with Reviewers" section.